

# Measuring Evolvability in Evolutionary Fuzzy Robotics

Seung-Ik Lee and Sung-Bae Cho  
Dept. of Computer Science, Yonsei University  
Seoul 120-749, South Korea  
cypher@candy.yonsei.ac.kr, sbcho@cs.yonsei.ac.kr

**Abstract** - This paper illustrates the evolutionary adaptive process of the rules of a fuzzy controller evolved by a genetic algorithm. Evolutionary activity and schema analysis are used to evaluate and analyze the evolution. The analysis shows that the evolution has been adaptive and final fuzzy rules have evolved from adaptive ones of earlier generations.

## I. INTRODUCTION

Much of previous work on evolutionary fuzzy logic controller (FLC) has shown successful results for the problems at hand. However, In-depth analysis on the role of evolutionary computation in finding the rules contained in the optimal controller has not been done seriously[1][2]. As there can be many evolutionary phenomena such as chances, necessity, random genetic drift, and adaptivity[3], a good evolutionary result cannot guarantee the re-occurrences of good solutions in following experiments even under the same conditions. To guarantee the success of evolution or at least raise the possibility of it requires higher level of capacity to produce adaptive candidate solutions that might drive evolution to success.

The capacity to produce good solutions via evolution, *evolvability*, can be defined in various ways as “genome’s ability to produce adaptive variants when acted on by the genetic system” by Wagner and Altenberg [4], “capacity to generate heritable phenotypic variation” by Kirshner and Gerhart [5], or “capacity to create new adaptations, and especially new kinds of adaptations, through the evolutionary process” by Bedau [6]. To obtain good solutions robustly, the evolvability should be maintained during the evolutionary process. Under this condition, good candidate solutions can contribute to the formation of the final solutions.

A promising way to measure evolvability, *evolutionary activity statistics*, was proposed by Bedau and Packard [6]. The method can measure evolvability in an objective and quantitative manner from data obtained by observing an evolving system. They applied these statistics to a variety of evolving systems for a variety of purposes [6][7]. However, they did not applied it to more realistic domains like evolutionary robotics.

In addition to measuring evolvability, we have realized that it is also important to reveal what evolutionary algo-

gorithms have done during evolution, especially on the evolutionary pathways to final solutions in order to understand evolutionary systems more completely. Revealing evolutionary pathways is to show the contributions of adaptive candidate solutions to the final solutions during evolution whereas measuring evolvability is to reveal the capability of generating new adaptive innovations to the solution space.

Therefore, this paper aims to show: 1) the role of evolutionary computation in finding the rules that are successful for solving problems by a measure of evolutionary activity proposed by Bedau and Packard [6]; 2) how the final solutions have evolved from earlier generations, *i.e.*, *evolutionary pathways*.

## II. EVolvABILITY MEASURE

Adaptability shows different characteristics compared to other genetic phenomena. Adaptive components in evolutionary systems generate innovative functional structures continuously and these structures persist in the systems because they have high adaptive behavioral characteristics. Therefore, if a system evolves adaptively, it means that the systems continuously generate new functional structures, which persist through the evolutionary process.

A counter,  $a_i(t)$ , of the  $i$ th component at time  $t$  is attached to each component of a system. A component’s activity changes over time as

$$a_i(t) = \sum_{k \leq t} \Delta_i(k) \quad (1)$$

where  $\Delta_i(k)$  is the activity increment for component  $i$  at time  $k$ . Various activity increment functions  $\Delta_i(t)$  can be used, depending on the nature of the components and the purposes at hand [6].

The number of components with activity  $a$  at time  $t$  is the *component activity distribution*,  $C(t, a)$  defined by

$$C(t, a) = \sum_i \delta(a - a_i(t)) \quad (2)$$

where  $\delta(a - a_i(t))$  is the Dirac delta function, equal to one if  $a = a_i(t)$  and zero otherwise. To measure the continual adaptive success of the components in the system at a give

time, *total cumulative evolutionary activity* or *total activity* in short,  $A_{cum}(t)$ , is defined by

$$A_{cum}(t) = \sum_i a_i(t) \rightarrow \int_0^\infty aC(t, a)da. \quad (3)$$

Dividing the cumulative evolutionary activity by diversity  $D(t)$  gives the cumulative activity per component, or *mean cumulative evolutionary activity* or *mean activity* in short, as follows:

$$\bar{A}_{cum}(t) = \frac{A_{cum}(t)}{D(t)} \quad (4)$$

where  $D(t)$  is the number of component  $i$  at time  $t$  with  $a_i(t) > 0$ .

Activity statistics most clearly reflect a system's adaptive evolutionary dynamics after they have been normalized by a 'neutral' model [8], to screen off the contribution of non-adaptive or maladaptive genotypes. This normalization can be used for several measures.

Adaptive innovations correspond to new components flowing into the system and proving their adaptive value through their persistent activity. *new evolutionary activity* or *new activity* in short,  $A_{new}(t)$ , is the reflection of the evolutionary adaptive innovations by summing the activity per component with values between  $a_0$  and  $a_1$  as (5) (i.e., a component  $i$  with  $a_0 < a_i(t) < a_1$  is regarded as adaptive innovation).

$$A_{new}(t) = \frac{1}{D(t)} \sum_{a=a_0}^{a_1} C(t, a) \rightarrow \frac{1}{D(t)} \int_{a_0}^{a_1} C(t, a)da. \quad (5)$$

### III. EVOLUTION OF FLC PARAMETERS

#### A. Khepera: Mobile robot

Khepera (see Fig. 1) was originally designed for research and teaching in the framework of a Swiss Research Priority Program [9]. It allows confrontation to the real world of algorithms developed in simulation for trajectory execution, obstacle avoidance, pre-processing of sensory information, and hypothesis test on behavior processing.

Fig. 1 (c) shows position of some parts of the robot. A Khepera robot has two wheels. A DC motor coupled with the wheel through a 25:1 reduction gear moves every wheel. An incremental encoder on the motor axis gives 24 pulses per revolution of the motor. This allows a resolution of 600 pulses per revolution of the wheel that corresponds to 12 pulses per millimeter of path of the robot. Eight infrared proximity sensors are placed around the robot and are positioned and numbered as shown in Fig. 1 (b). These sensors embed an infrared emitter and a receiver.

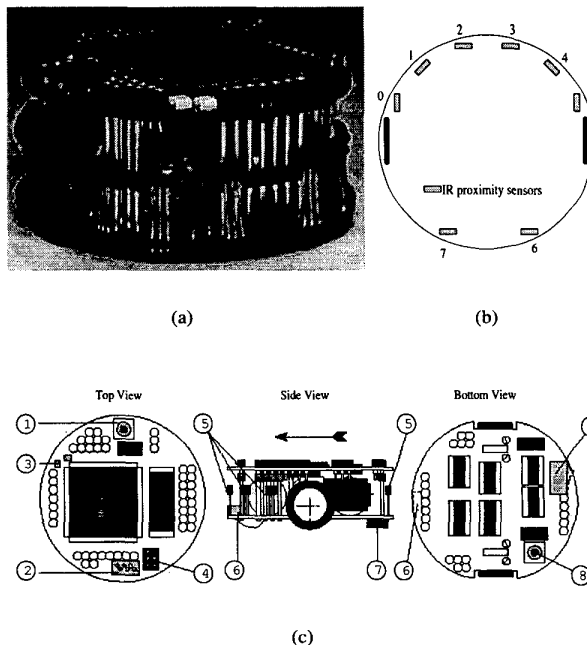


Fig. 1. (a) Mobile robot. (b) Position of the 8 IR sensors. (c) 1) LEDs. 2) Serial line (S) connector. 3) Reset button. 4) Jumpers for the running mode selection. 5) Infra-Red proximity sensors. 6) Battery recharge connector. 7) ON-OFF battery switch. 8) Second reset button.

#### B. Evolution

Two parameters should be determined to run a genetic algorithm (GA) [10]: how to encode the FLC parameters in gene code and how to estimate the fitness value of each individual. For the FLC parameters, an individual is encoded to have eight input variables, two output variables, and maximally twenty rules shown in Fig. 2. Each rule in an individual shares the variables.

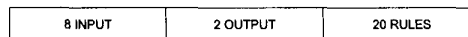


Fig. 2. Gene representation of an individual

Each variable in Fig. 2 encode fuzzy membership functions defined on it. Though we have defined 5 fuzzy sets in a variable, only three of their membership functions need to be encoded as in Fig. 3 because the other two have fixed center position.

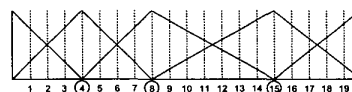


Fig. 3. Encoding of membership functions of a variable

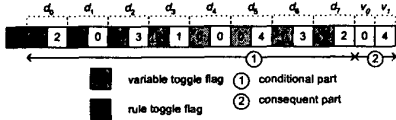


Fig. 4. Encoding of a rule

Each rule has eight input variables,  $d_0, \dots, d_7$ , and two output variables,  $v_0$  and  $v_1$ . Variables having the toggle bit 1 participate in the conditional part in a fuzzy rule. Output variables do not have a toggle flag because all of them should appear in the consequent part. The first bit in Fig. 4 designates whether this rule participates in fuzzy inference process or not. Therefore, Fig. 4 can be decoded as follows:

IF ( $d_0 = M$ ) and ( $d_1 = VF$ ) and ( $d_6 = C$ ) and ( $d_7 = M$ )  
THEN ( $v_0 = BF$ ) and ( $v_1 = FF$ )

The fitness of an individual,  $\Theta$ , with  $s$  run time steps and  $n$  check-points passed through is defined by

$$\Theta = \left(\frac{n}{N}\right) \sum_{t=0}^s V_t (1 - \sqrt{D_t}) (0.5 + 0.5(1 - I_t)) \quad (6)$$

where  $N$  is total number of check-points,  $V_t$  is average rotational speed at step  $t$ ,  $D_t$  is the normalized absolute value of the difference between the speed of the two wheels, and  $I_t$  represents the normalized value of the sensor which presents the highest level of activation.

For more information on the parameters of fuzzy logic controller of this paper, refer to [2].

### C. Experimental Setup

A genetic algorithm was used for the evolution of fuzzy rules. In the beginning of evolution, we initialized 50 individuals randomly. Maximum generation was 1000. Population was overlapped by 50% with elitist strategy. Individuals with relatively low fitness values were replaced by new individuals. Crossover rate was set 0.5 and mutation rate was 0.01.

We also experimented a neutral shadow of the fuzzy model to identify the extent to which a system's evolutionary dynamics depend on adaptation rather than other evolutionary forces like chance and necessity according to Reichtsteiner and Bedau [7]. That is, we screen off the effect of non-adaptive evolutionary forces by comparing the evolutionary dynamics observed in target evolutionary systems with those observed in analogous evolutionary systems in which adaptive evolution cannot happen. Filtering observed data with a neutral model yields a measure of excess evolutionary activity. In effect, neutral models are null hypotheses against which the action of adaptive evolution stands out in relief.

As the number of whole rules in a population is constant, a rule's relative significance is expressed by the number or ratio of the rule's genotype. Therefore, the evolutionary activity  $a_i(t)$  of the  $i^{th}$  genotype at time  $t$  is defined as its instances integrated over the time period from its origin up to  $t$ , provided it exists:

$$a_i(t) = \begin{cases} \int_0^t n_i(t) dt & \text{if genotype } i \text{ exists at } t \\ 0 & \text{otherwise.} \end{cases} \quad (7)$$

where  $n_i(t)$  is the number of rules that has  $i^{th}$  genotype at  $t$ .

### D. Simulation Results

Fig. 5 (a) shows fitness changes over generation of the simulation. Average fitness increases slowly as generation goes by and best fitness increases over generation with some oscillations. However, after about the 550th generation, the best fitness increases dramatically with high oscillations. In general, best fitness does not oscillate with elitist strategy if the test field or environment does not change over time. Because the sensory inputs have about 10% noises for more realistic simulation, fitness values of the same FLC may vary depending on sensory inputs as in Fig. 5 (a).

From the 554th generation, individuals of extremely high fitnesses start to show up and disappear. The best that reaches the goal has appeared at generation 746. The movements of the best individual is shown in Fig. 5 (b). As you see, the best individual shows behaviors like "left turn," "right turn," "passing through narrow corridor," and "moving in wide area," which we did not specify in the gene code.

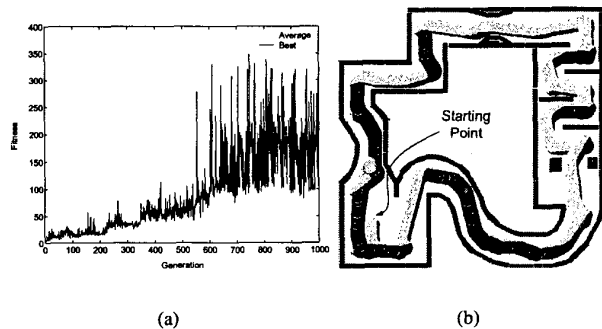


Fig. 5. (a) Fitness changes (b) Trajectory of the best individual

The best individual shown in Fig. 5 (b) has 13 effective rules (*i.e.*, the rules that have rule toggle flag on in the gene code) and uses only seven out of the 13 rules. During the steps shown in Fig. 5 (b), rules  $R_8$ ,  $R_{10}$ , and  $R_{11}$  are used more frequently than the other rules.

## IV. EVOLVABILITY IN FUZZY ROBOTICS

### A. Measurement of Adaptability

In this section, we will show that the performance shown by the best individual is the result of adaptation to the given problem by utilizing the concept of evolutionary activity proposed by Bedau [6]. Fig. 6 shows the component activity distribution function. This graphs depict how evolutionary activity of the rules on the  $y$ -axis varies as a function of time on the  $x$ -axis. There are myriad lines or waves evident in Fig. 6. Each wave corresponds to a single rule and shows the variation over time of that rule's evolutionary activity.

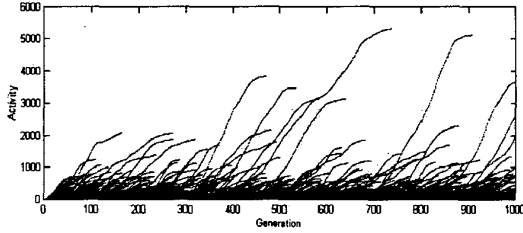


Fig. 6. Activity distribution function  $C(t, a)$

By the definition of evolutionary activity as (1), the slope of a given rule's activity wave at a given time can be interpreted as the rule's concentration in the population at that time because the number of all rules in a population at a time is constant. When a new rule enters the population, a new wave arises from the  $x$ -axis. As the rule's concentration in the population grows (or shrinks) over time, the slope of the wave increases (or decreases). When the rule finally goes extinct, the slope of its wave falls to zero and the wave ends. In this way, a rule's activity wave reflects its changing concentration throughout its history in the population. Whenever one rule drives another to extinction, a new wave arises as an earlier one dies out. The dominating rules during a given epoch of evolution appear as dominating waves.

Fig. 7 (a) shows the time series of diversity  $D$ . The neutral shadow's diversity values are pretty much higher than those of the fuzzy model. This arises from the fact that there is no selective pressure in the neutral shadow model in contrast to the fuzzy model, where more adaptive individuals have higher possibilities of being selected and, therefore, produce more children and persist over time.

Fig. 7 (b) shows mean cumulative evolutionary activity,  $\bar{A}_{cum}$ , of the two models.  $A_{cum}$  and  $\bar{A}_{cum}$  are significantly higher in the fuzzy model than in the neutral shadow. This means that much more adaptive rules are present in the fuzzy model than in its neutral shadow.

Fig. 7 (c) illustrates the difference of the component activity distributions between the fuzzy model and its neutral shadow. The distributions shown in Fig. 6 have been summed along the temporal dimension and then divided by

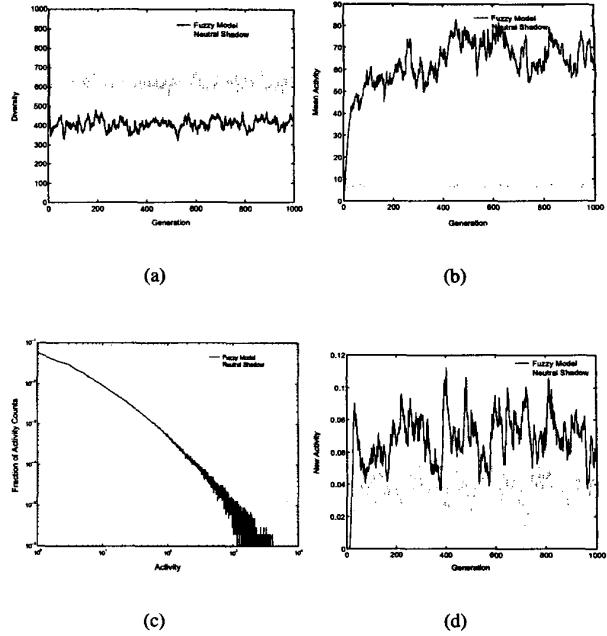


Fig. 7. (a) Diversity  $D(t)$  (b) Mean cumulative evolutionary activity  $\bar{A}_{cum}(t)$  (c) Log-log plot of the component activity distributions for the fuzzy model and its neutral shadow (d) New activity  $A_{new}(t)$

the total number of counts in both distributions. Therefore, the value of each distribution at a given activity value  $a$  represents the fraction of activity counts in each distribution that have activity  $a$ . As you can see in Fig. 7 (c), the fraction of activity counts of neutral shadow at relatively lower activities is higher than that of the fuzzy model. However, at higher activities, the fraction of activity counts of neutral shadow is much lower than that of the fuzzy model. This means that high adaptive rules are much more in the fuzzy model than in its neutral shadow.

The point at which the two distributions have the same value,  $a'$ , is an activity count that is equally likely to have been chosen from either distribution. This value is used to calculate new activity,  $A_{new}$ , with  $a_0$  to be  $a'$  and  $a_1$  slightly above  $a'$  as follows:

$$a_1 = a' + (0.05 \times (a_{max} - a')) \quad (8)$$

where  $a_{max}$  is the highest activity value at which either distribution is positive and  $a'$  is the lowest value at which the two distributions cross. Since the lowest value at which two distributions cross in Fig. 7 (c) is  $a' = 145$  and  $a_{max} = 5.313 \times 10^3$ , we set  $a_0 = a' = 1.45 \times 10^1$  and  $a_1 = 4.03 \times 10^1$  respectively.

With these values, we can calculate new activity as in Fig. 7 (d). The new activity values of the fuzzy model is higher than that of the neutral shadow, which means that

new activity signaling the positive adaptability flows more frequently into the fuzzy model compared to that of the neutral shadow. Therefore, we can conclude from this figure that the fuzzy model continuously generates new adaptive fuzzy rules much more than the neutral shadow does.

**B. Analysis of the Best Individual**

In previous sections, we have analyzed the behavioral properties of some salient rules. The salient rules have important behavioral properties like “turn left,” “turn right,” and “move forward.” As these behaviors are important for the robot to safely navigate in the environment, they are much more adaptive than other behaviors or rules. In this section, we illustrate that these adaptive behaviors or rules contribute to the construction of the best individual we briefly described in previous section. For this purpose, we utilize schema analysis and evolutionary activities of the schemata of both the salient rules and the rules of the best individual. Note that, from now on, we name the schema of a rule  $R_n$  as  $R_{\{n\}}$  by surrounding the rule number with braces.

TABLE I  
SCHEMATA OF THE SALIENT RULES

Rule	Gene Code	Schema
S <sub>1</sub>	1030202010010031113	#####10##1113
S <sub>2</sub>	1011010040004010344	###1010#####44
S <sub>3</sub>	1031010040002010344	
S <sub>7</sub>	1001010040002010344	
S <sub>12</sub>	1011010040002010344	
S <sub>4</sub>	1030200011100031113	#####11####1113
S <sub>5</sub>	1030201041401010041	#####14#####41
S <sub>8</sub>	1000201011401010041	
S <sub>6</sub>	1021410030404030401	###1410#####01
S <sub>9</sub>	1100201011401010341	#10#####14#####41
S <sub>11</sub>	1100001011401010341	
S <sub>10</sub>	1000404040202031102	#####11102

TABLE I shows the gene codes and their corresponding schemata of the salient rules and TABLE II shows the gene codes and their corresponding schemata of the rules of the best individual. Each schema is obtained by masking off the alleles that does not actually participate in the conditional part of the rule. This can be identified by looking at the “variable toggle flag” shown in Fig. 4. Comparing the two tables gives direct connections among schemata.  $B_{\{6\}}$  are the same with schema  $S_{\{10\}}$ , and schema  $B_{\{10\}}$  is also the same with schema  $S_{\{2,3,7,12\}}$ .

**Analysis of the Best Individual’s Rule B<sub>2</sub>:** The construction pathway of the rule B<sub>2</sub> can be inferred from the comparison of its schema with others’. Comparing schema B<sub>2</sub> with S<sub>1</sub> and S<sub>4</sub> reveals that there are similarities among

TABLE II  
SCHEMATA OF THE RULES OF THE BEST INDIVIDUAL

Rule	Gene Code	Schema
B <sub>2</sub>	1010303111203001133	#####1112####1133
B <sub>6</sub>	1000200030100031102	#####1102
B <sub>7</sub>	1021411000404110401	###1411#####11##01
B <sub>10</sub>	1001010040002020044	###1010#####44
B <sub>11</sub>	1100201041401011041	#10#####14####1041
B <sub>15</sub>	1121300101102021022	#1213##1011####1022
B <sub>18</sub>	1041302040003120021	###13#####12##21

them. Schema S<sub>1</sub> originates at the beginning of evolution and has many instances up to about 240th generation. S<sub>4</sub> originates at 285th generation and persists up to 600th generation.

Fig. 8 shows the activities of the instances of each schema. As you can see, the extinction or decrease of schema S<sub>1</sub> leads to the origination or increase of S<sub>4</sub>. The extinction or decrease of schema S<sub>4</sub> also leads to the origination or increase of schema B<sub>2</sub>.

From this inspection, we can infer that the origination of B<sub>2</sub> at generation 730 is caused by certain genetic operations, “cross over” or “mutation,” on one of the genotypes of schema B<sub>2</sub> originated at 654th generation. This schema B<sub>2</sub> originates from schema S<sub>4</sub>, which also originates from schema S<sub>1</sub> at about 280 generation. Schema S<sub>1</sub> originates at the beginning of evolution. Therefore, the rule B<sub>2</sub> is the result of continuous genetic modifications of one of the rules at generation 0 and its adaptive capabilities.

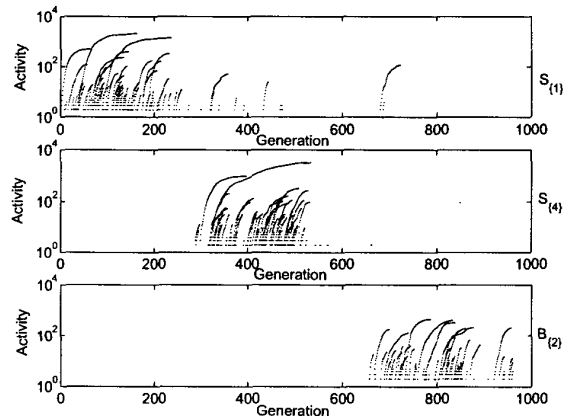


Fig. 8. Activities of different instances of schemata S<sub>1</sub>, S<sub>4</sub>, and B<sub>2</sub>

**Analysis of the Best Individual’s Rule B<sub>7</sub>:** In TABLE II, we can find schema B<sub>7</sub> is very similar to schema S<sub>6</sub>. The

number of instances of schema  $S_{\{6\}}$  increases after 350th generation and decreases after 650th generation, whereas that of schema  $B_{\{7\}}$  increases from 650th generation (see Fig. 9).

From this inspection, we can infer that the origination of  $B_7$  at generation 678 is caused by certain generic operations, "cross over" or "mutation" on one of the genotypes of schema  $B_{\{7\}}$ , which originates at 651st generation. Schema  $B_{\{7\}}$  originates from schema  $S_{\{6\}}$ , which originates at 195th generation. Therefore, rule  $B_7$  is the result of continuous genetic modifications of one of the rules at generation 195 and its adaptive capabilities.

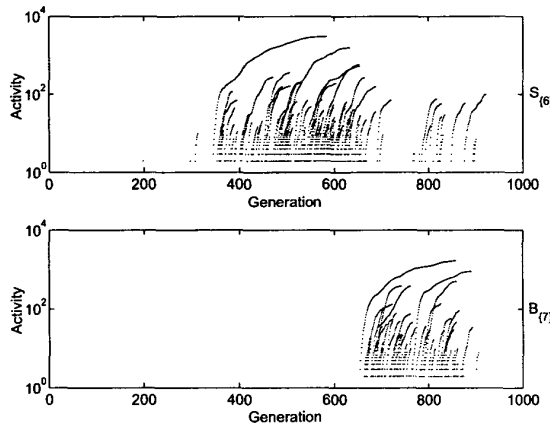


Fig. 9. Activities of different instances of schemata  $S_{\{6\}}$  and  $B_{\{7\}}$

**Analysis of Best Individual's Rule  $B_{11}$ :** The construction pathway of rule  $B_{11}$  can be inferred from the inspection of its schema. In TABLE II, schema  $B_{\{11\}}$  is very similar to schema  $S_{\{5,8\}}$  and  $S_{\{9,11\}}$ . Fig. 10 shows the changes of the number of genotypes of each schema  $S_{\{5,8\}}$ ,  $S_{\{9,11\}}$ , and  $B_{\{11\}}$ , and their related evolutionary activities. From this figure, we can infer that  $S_{\{9,11\}}$  originates from  $S_{\{5,8\}}$  as a subset and  $B_{\{11\}}$  originates from schema  $S_{\{9,11\}}$  as a subset.  $B_{\{11\}}$  leads to the origination of rule  $B_{11}$  at generation 741.

As a summary, we can infer that most of the rules of the best individual,  $B_2$ ,  $B_6$ ,  $B_{10}$ , and  $B_{11}$ , are not the results of chances or other genetic phenomena, but the results of their adaptive capabilities. The other rules of the best individual,  $B_{15}$  and  $B_{18}$ , originate just before the origination of the best individual and extinguish after a few generations because these rules do not show adaptive behaviors.

## V. CONCLUSION

In this paper, we have quantified the evolution of a fuzzy controller for a mobile robot and shown that the rules of the best individual are the result of their adaptive capabilities. Furthermore, we also have illustrated the evolutionary construction pathways of the rules of the best individual by analyzing the schemata of the best individual's rules and salient

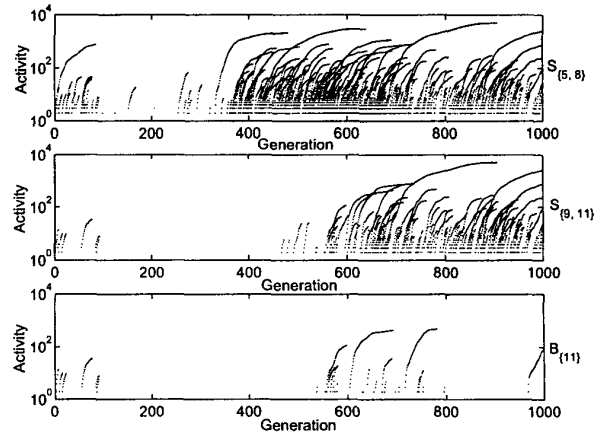


Fig. 10. Activities of different instances of schema  $S_{\{5,8\}}$ ,  $S_{\{9,11\}}$ , and  $B_{\{11\}}$

rules.

The evolutionary activities have shown that the performance of the best individual is not the results of other genetic phenomena such as chances or random genetic drift, but the results of their adaptabilities. Schema analysis has shown that most of the rules of the best individual have been prepared at the earlier stage of evolution and proven adaptive for a long time over generation.

Therefore, we can conclude that the evolved fuzzy controller is the results of adaptive evolution and the evolutionary activity and schema analysis prove to be useful for quantifying adaptability and showing evolutionary construction pathways.

## References

- [1] K. Izumi, K. Watanabe, and T. Miyazaki, "Fuzzy behavior-based control for a miniature mobile robot," *Proceedings of Knowledge-Based Electronic Systems*, vol. 3, pp. 483-490, 1998.
- [2] S.-I. Lee and S.-B. Cho, "Emergent behaviors of a fuzzy sensor-motor controller evolved by genetic algorithm," *IEEE Transactions on System, Man, and Cybernetics: Part B*, vol. 31, no. 6, pp. 919-929, 2001.
- [3] M.J. West-Eberhard, "Adaptation: current uses," *Keywords in Evolutionary Biology*, Harvard University Press, pp. 13-18, 1992.
- [4] G.P. Wagner and L. Altenberg, "Complex adaptations and the evolution of evolvability," *Evolution*, vol. 50, pp. 967-976, 1996.
- [5] M. Kirschner and J. Gerhart, "Evolvability," *Proc. Nat. Acad. Sci.*, vol. 95, pp. 8420-8427, 1998.
- [6] M.A. Bedau and N.H. Packard, "Measurement of evolutionary activity, teleology, and life," *Artificial Life 2*, Addison-Wesley, Redwood City, pp. 431-461, 1992.
- [7] A. Rechtsteiner and M.A. Bedau, "A generic neutral model for measuring excess evolutionary activity of genotypes," *Proceedings of the Genetic and Evolutionary Computation Conference*, vol. 2, pp. 1366-1373, 1999.
- [8] M.A. Bedau, E. Snyder, and N.H. Packard, "A classification of long-term evolutionary dynamics," *Artificial Life 6*, pp. 228-237, 1998.
- [9] K-Team, *Khepera Simulator Version 5.02 User Manual*, <http://www.k-team.com/download/khepera.html>, 1999.
- [10] D.E. Goldberg, *Genetic Algorithms in Search, Optimization & Machine Learning*, Addison Wesley, 1989.